

# Metal slit array Fresnel lens for wavelength-scale optical coupling to nanophotonic waveguides

Young Jin Jung, Dongwon Park, Sukmo Koo, Sunkyu Yu, and Namkyoo Park\*

Photonic Systems Laboratory, School of EECS, Seoul National University, Seoul 151-744, Korea  
\*nkpark@snu.ac.kr

**Abstract:** We propose a novel metal slit array Fresnel lens for wavelength-scale optical coupling into a nanophotonic waveguide. Using the plasmonic waveguide structure in Fresnel lens form, a much wider beam acceptance angle and wavelength-scale working distance of the lens was realized compared to a conventional dielectric Fresnel lens. By applying the plasmon waveguide dispersion relation to a phased antenna array model, we also develop and analyze design rules and parameters for the suggested metal slit Fresnel lens. Numerical assessment of the suggested structure shows excellent coupling efficiency (up to 59%) of the 10  $\mu\text{m}$  free-space Gaussian beam to the 0.36  $\mu\text{m}$  Si waveguide within a working distance of a few  $\mu\text{m}$ .

©2009 Optical Society of America

**OCIS codes:** (240.6680) Surface plasmons; (140.3325) Laser coupling; (080.3620) Lens system design

---

## References and links

1. K. F. MacDonald, Z. L. Samson, M. I. Stockman, and N. I. Zheludev, "Ultrafast active plasmonics," *Nat. Photonics* **3**(1), 55–58 (2008).
2. S. Yu, S. Koo, and N. Park, "Coded output photonic A/D converter based on photonic crystal slow-light structures," *Opt. Express* **16**(18), 13752–13757 (2008).
3. M. T. Hill, Y. S. Oei, B. Smalbrugge, Y. Zhu, T. D. Vries, P. J. V. Veldhoven, F. W. M. V. Otten, T. J. Eijkemans, J. P. Turkiewicz, H. De Waardt, E. J. Geluk, S. H. Kwon, Y. H. Lee, R. Notzel, and M. K. Smit, "Lasing in metallic-Coated nanocavities," *Nat. Photonics* **1**(10), 589–594 (2007).
4. L. Vivien, S. Laval, E. Cassan, X. L. Roux, and D. Pascal, "2-D taper for low-loss coupling between polarization-insensitive microwaveguides and single-mode optical fibers," *J. Lightwave Technol.* **21**(10), 2429–2433 (2003).
5. L. Pavesi, and G. Guillot, *Optical Interconnects: The Silicon Approach* (Springer, 2006).
6. B. L. Miao, C. H. Chen, S. Y. Shi, and D. W. Prather, "A high-efficiency in-plane splitting coupler for planar photonic crystal self-collimation devices," *IEEE Photon. Technol. Lett.* **17**(1), 61–63 (2005).
7. D. W. Prather, J. Murakowski, S. Y. Shi, S. Venkataraman, A. Sharkawy, C. H. Chen, and D. Pustai, "High-efficiency coupling structure for a single-line-defect photonic-crystal waveguide," *Opt. Lett.* **27**(18), 1601–1603 (2002).
8. F. J. Garcia-Vidal, L. Martin-Moreno, H. J. Lezec, and T. W. Ebbesen, "Focusing light with a single subwavelength aperture flanked by surface corrugations," *Appl. Phys. Lett.* **83**(22), 4500 (2003).
9. C. Genet, and T. W. Ebbesen, "Light in tiny holes," *Nature* **445**(7123), 39–46 (2007).
10. F. J. Garcia-Vidal, H. J. Lezec, T. W. Ebbesen, and L. Martin-Moreno, "Multiple paths to enhance optical transmission through a single subwavelength slit," *Physical Review Letters* **90**, - (2003).
11. N. Yu, R. Blanchard, J. Fan, Q. J. Wang, C. Pflügl, L. Diehl, T. Edamura, M. Yamanishi, H. Kan, and F. Capasso, "Quantum cascade lasers with integrated plasmonic antenna-array collimators," *Opt. Express* **16**(24), 19447–19461 (2008).
12. T. Ishi, J. Fujikata, K. Makita, T. Baba, and K. Ohashi, "Si nano-photodiode with a surface plasmon antenna," *Japanese Journal of Applied Physics Part 2-Letters & Express Letters* **44**, 364–366 (2005).
13. N. F. Yu, J. Fan, Q. J. Wang, C. Pflügl, L. Diehl, T. Edamura, M. Yamanishi, H. Kan, and F. Capasso, "Small-divergence semiconductor lasers by plasmonic collimation," *Nat. Photonics* **2**(9), 564–570 (2008).
14. H. F. Shi, C. T. Wang, C. L. Du, X. G. Luo, X. C. Dong, and H. T. Gao, "Beam manipulating by metallic nano-slits with variant widths," *Opt. Express* **13**(18), 6815–6820 (2005).
15. Z. J. Sun, "Beam splitting with a modified metallic nano-optic lens," *Appl. Phys. Lett.* **89**, - (2006).
16. H. X. Yuan, B. X. Xu, and T. C. Chong, "Focusing effect and performance analysis of flat metal slit array lens," in *Optical Data Storage*(2007), p. TuE2.
17. H. X. Yuan, B. X. Xu, B. Lukiyanchuk, and T. C. Chong, "Principle and design approach of flat nano-metallic surface plasmonic lens," *Applied Physics Materials Science & Processing* **89**(2), 397–401 (2007).

18. Z. J. Sun, and H. K. Kim, "Refractive transmission of light and beam shaping with metallic nano-optic lenses," *Appl. Phys. Lett.* **85**(4), 642–644 (2004).
  19. T. Xu, C. L. Du, C. T. Wang, and X. G. Luo, "Subwavelength imaging by metallic slab lens with nanoslits," *Applied Physics Letters* **91**, - (2007).
  20. M. K. McGaugh, C. M. Verber, and R. P. Kenan, "Modified Integrated-Optic Fresnel Lens for Wave-Guide-to-Fiber Coupling," *Appl. Opt.* **34**(9), 1562–1568 (1995).
  21. C. A. Balanis, *Antenna theory: analysis and design* (Wiley-Interscience, 2005).
  22. R. Qiang, R. L. Chen, and J. Chen, "Modeling electrical properties of gold films at infrared frequency using FDTD method," *Int. J. Infrared Millim. Waves* **25**(8), 1263–1270 (2004).
  23. A. D. Rakic, A. B. Djuricic, J. M. Elazar, and M. L. Majewski, "Optical properties of metallic films for vertical-cavity optoelectronic devices," *Appl. Opt.* **37**(22), 5271–5283 (1998).
  24. J. M. Helt, C. M. Drain, and G. Bazzan, "Stamping patterns of insulated gold nanowires with self-organized ultrathin polymer films," *J. Am. Chem. Soc.* **128**(29), 9371–9377 (2006).
- 

## 1. Introduction

There has been unprecedented progress in the field of nanophotonics over the last decade. By using photonic crystals and plasmonics, or by employing silicon photonics, much progress has been made for nanophotonic functional devices to be used in future photonic circuits and photonic signal processing. The motivation behind nanophotonics is twofold: to overcome the bottleneck encountered in ultra-high speed integrated electronic circuits, and at the same time to reduce the footprint of today's conventional photonic devices. Achievements have been realized for nanophotonic devices in terms of operational speed [1], functionality [2], and decreased size [3]. However, the problem of coupling these nanophotonic structures to the external world (e.g., fiber, conventional dielectric waveguides, or free-space) has received less attention than the nanophotonic devices themselves. Summarizing the current efforts, the nanophotonic coupling structures, in terms of their operating principles, can be classified as follows: a) adiabatic, such as taper, inverse taper, and graded index taper [4]; b) evanescent; c) ray optics using a microlens or mirror; and d) combinations of these.

Still, with their inherent limitations, the reported coupling length based on adiabatic or evanescent methods usually must remain in the tens-of-micrometers regime. For example, tapering (or inverse tapering) structures of waveguide couplers [4] often extends to almost the millimeter scale. For adiabatic couplers, the taper length should be much larger than the beat length between the fundamental mode and dominant coupling mode [5]. For an evanescent coupler, the interaction length needs to be large enough to guarantee efficient power transfer [5]. At last, *focal length* of micrometers scale could be realized utilizing ray optic approaches, but including the thickness of the microlens, the *coupling length* of the ray optic coupler device must remain in the regime of tens-of-micrometers [6,7].

Whereas the footprints of those to-be-coupled nanophotonic devices can be realized within tens of micrometers in size, the feature size of waveguide couplers thus extends to almost the millimeter scale at current situation. Considering the recent advent of plasmonics, the realization of a wavelength scale coupler should be feasible if we consider the well-accepted idea of an optical antenna.

In this paper we investigate the feasibility of using a plasmonic Fresnel lens instead of a conventional microlens for the reduction of the lens footprint in the ray-optic platform. Identifying the difficulties associated with dielectric Fresnel lens coupling in extremely high numerical aperture (NA) applications, we propose a nanophotonic metallic Fresnel lens, based on metallic plasmon slit [8–13] (or array [14–19]) structures. We show that it is possible to overcome the limitation of the dielectric Fresnel lens (with respect to the acceptance angle as dictated by Snell's law) utilizing plasmon propagation inside the metal slits, instead of light propagation in the dielectric lens. Based on phase antenna array formalism, design principles for the metallic Fresnel lens will be derived, and performance comparisons will be made against dielectric Fresnel lens using finite difference time domain (FDTD) numerical analysis.

## 2. Theory

For the current study, we restrict our application examples to two-dimensional (or slab) structures. Setting the target focal length of the device to 1.5  $\mu\text{m}$  (the same as the wavelength

used in the study, 1550nm), we consider the case of direct beam coupling from the free space (a spot size of 10  $\mu\text{m}$ ) into the 0.36  $\mu\text{m}$ -wide silicon waveguide. First, to study the performance of the dielectric Fresnel lens, the detail of the structure shown in Fig. 1(a) was determined following the approach explained in [20]. A solid immersion lens with silicon was assumed to minimize the beam width entering the coupling waveguide.

With the extreme mismatch in the dimensions of the incident beam width and the coupling waveguide (10  $\mu\text{m}$  to 0.36  $\mu\text{m}$ ), combined with the severe constraint for a focal length as short as 1.5  $\mu\text{m}$ , the light entering from the off-center part of the lens (higher-order Fresnel zone) resulted in total internal reflection at the silicon-air boundaries (solid blue line in the figure) of the dielectric Fresnel lens (Fig. 1a). This reflection phenomenon for the dielectric Fresnel lens in wavelength scale coupling causes a significant loss in the coupling efficiency, as confirmed by the FDTD analysis. As can be observed, Fig. 3(a) shows the diverging refracted beam at the exit of the lens.

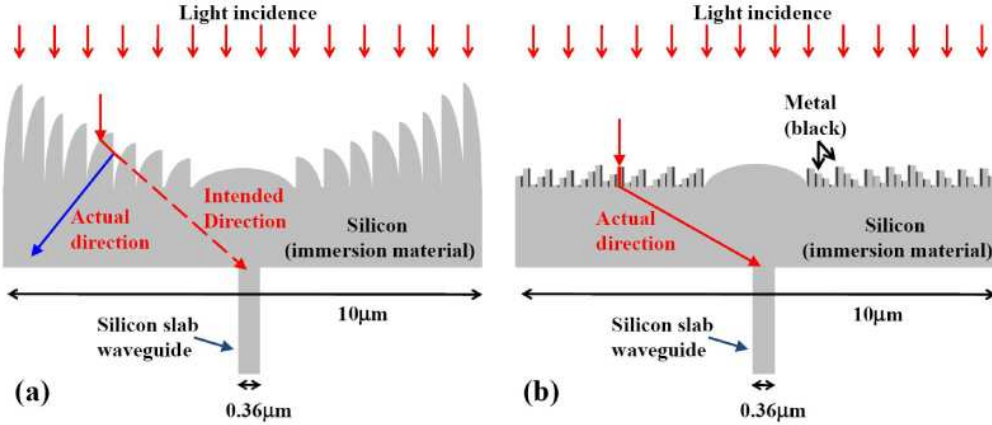


Fig. 1. Structure of the (a) silicon Fresnel lens coupler, and (b) metal slit array Fresnel lens coupler. Propagation paths of the light are shown with a dotted line (ideal path) and solid line (actual path).

This observed problem of the reflection of light entering the dielectric Fresnel lens can be mitigated using our proposed structure as shown in Fig. 1(b). By exciting plasmons at the lens entrance, then guiding waves with the metal-insulator-metal (MIM) waveguides, and finally regenerating point sources at the exit of the MIM waveguides, now one simply need consider the propagation delay between the source and focal point without any reflection from the dielectric / free space interface of the Fresnel lens.

For the determination of the metallic Fresnel lens structure, we utilize the theory of the phased array antenna [21], which has been implemented for photonic devices of various functionalities [14–19]. Figure 2 shows the zoomed-in view of the metallic Fresnel lens with related design parameters. Worth to note, for the 0th-order Fresnel lens, we assume a dielectric lens, to minimize the metallic loss. Assuming a plane wave of incidence, the accumulated phase shift of the beam at the entrance to the coupling waveguide can be easily calculated. The phase matching condition at the coupling waveguide then becomes

$$\begin{aligned}\beta_2(l_0 + l_f) &= \beta_1(l_0 - l_s) + \beta_2\sqrt{(l_s + l_f)^2 + d_s^2} + 2\pi \cdot M \\ &= \beta_1(l_0 - l_p) + \beta_3l_p + \beta_2\sqrt{l_f^2 + d_p^2} + 2\pi \cdot N\end{aligned}\quad (1)$$

where  $l_f$ ,  $l_0$ ,  $l_s$ , and  $l_p$  are the focal length from the emitting surface of the lens, the thickness of the 0th-order Fresnel silicon lens at the center, the thickness of the 0th-order Fresnel silicon lens at  $r = d_s$ , and the length of the MIM plasmonic waveguide, respectively.  $\beta_1$ ,  $\beta_2$ , and  $\beta_3$  are the propagation constants of free space, silicon, and the MIM waveguide of dielectric width

$w_d$ , respectively, and  $M$  and  $N$  are integers. To calculate the propagation constant  $\beta_3$  of the plasmon in the MIM waveguide in our structure, we use the following relation [16]:

$$\tan h(\sqrt{\beta_3^2 - k_0^2 \epsilon_d} w_d / 2) = \frac{-\epsilon_d \sqrt{\beta_3^2 - k_0^2 \epsilon_m}}{\epsilon_m \sqrt{\beta_3^2 - k_0^2 \epsilon_d}} \quad (2)$$

where  $k_0$  is the wave vector in free space;  $\epsilon_d$  and  $\epsilon_m$  are the relative permittivities for the insulator and metal respectively; and  $w_d$  is the width of the insulator between metal layers. In our design, gold ( $\epsilon_m = -140 + 10i$  at 1550 nm [22]) and silicon ( $\epsilon_m = 3.5^2$ ) have been assumed as the metal and dielectric. Solving Eqs. (1) and (2) simultaneously with preset fixed values of  $l_0$ ,  $w_d$ , and  $w_m$ , we then calculate  $l_s$  and  $l_p$  to finalize the metallic Fresnel lens design.

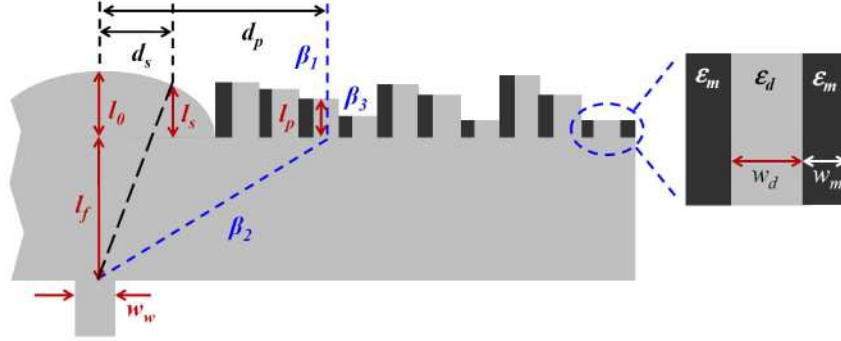


Fig. 2. Design parameters of the metal slit array Fresnel lens coupler. Inset shows a zoomed-in view of the MIM surface plasmon waveguide.  $\beta_1$ ,  $\beta_2$ , and  $\beta_3$  are the propagation constants of free space, silicon, and the MIM waveguide.  $w_i$ : width of waveguide ( $w$ ), metal ( $m$ ), dielectric ( $d$ )

### 3. Results

Setting the dimensions of the MIM waveguide to  $w_d = 100$  nm,  $w_m = 50$  nm, then  $\beta_3$ ,  $l_0 = 475$  nm (set by  $\max[l_p] = 2\pi/(\beta_3 - \beta_1)$ ),  $l_s$  and  $l_p$  of the Fresnel lens were calculated to give the minimum (limited by the numerical aperture of silicon) focal length  $l_f$  of 1.5  $\mu\text{m}$  at  $\lambda = 1.55$   $\mu\text{m}$ . To verify the operation of the lens, a 2-D FDTD calculation was carried out for the proposed coupling structure. A Gaussian input beam with a 10  $\mu\text{m}$  spot size was applied from free space into the metallic Fresnel lens, and then into the 0.36  $\mu\text{m}$  silicon single mode waveguide. The coupling efficiency of the lens was calculated by measuring the flux integrated over the cross section region of 0.36  $\mu\text{m}$  waveguide (at the far end of the coupler) divided by the incident plane wave power at the entrance of the metallic Fresnel lens. Figure 3 shows the FDTD calculation results of the designed coupling structures for (a) the silicon Fresnel lens, and (b) the metal slit array Fresnel lens. The working distance (thickness of the lens plus focal length) and coupling efficiency of each lens were 4  $\mu\text{m}$  and 23% for the silicon Fresnel lens, and 2  $\mu\text{m}$  and 45% for the metallic Fresnel lens, respectively. As can be seen from the figures, diverging beams from the silicon Fresnel lens are evident; which cause lower coupling efficiency for the silicon Fresnel lens.

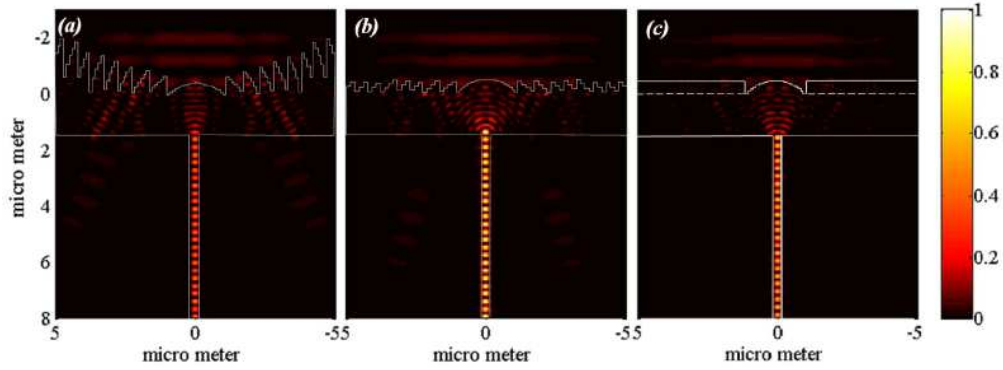


Fig. 3. Plot of the Poynting vector magnitude for (a) silicon Fresnel lens, and (b) metallic Fresnel lens ( $w_d = 100$  nm,  $w_m = 50$  nm). (c) metallic lens with variant width [14]. Gray lines show the outline of each lens structure and coupling Si waveguide ( $w_w = 0.36$   $\mu\text{m}$ )

To study the effect of MIM waveguide loss as well as possible mode coupling between the MIM waveguides, MIM waveguides with different dielectric widths  $w_d$  and MIM waveguide pairs with different metal barrier widths  $w_m$  were tested.

Figures 4(a) and (b) show the propagation of the wave in the MIM waveguide at  $w_d = 10$  nm and 50 nm, respectively. As expected based on Eq. (2), significant waveguide attenuation was observed for the MIM waveguide with  $w_d < 20$  nm, where the imaginary part of the propagation constant  $\beta_3$  became too large for the given length of the waveguide. Using a fixed loss-minimized MIM width  $w_d$ , and also by using Fresnel phase rotation for much shorter waveguide length, our implementation provides much higher coupling throughput efficiency (45%) than what is reported in [14] (Fig. 3(c), 33%). Figure 4(c) also shows the interference between the MIM waveguides when the width of the metal barrier  $w_m$  became too small (less than the skin depth of gold  $\sim 25$  nm, at 1550 nm [23]).

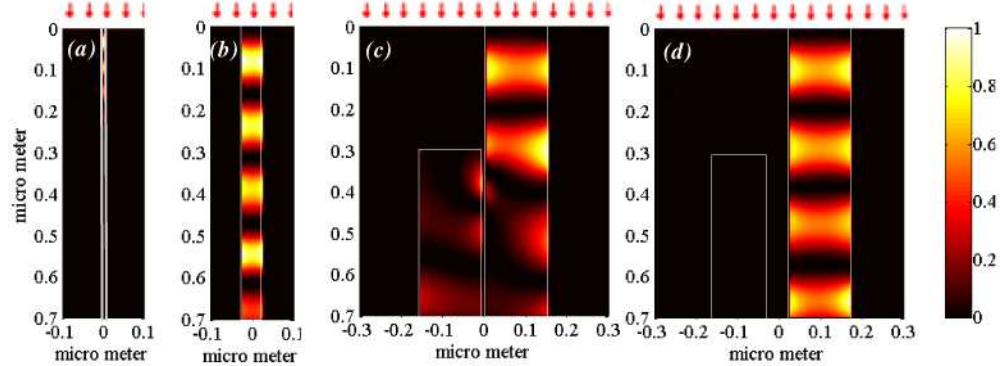


Fig. 4. Propagation of the wave in MIM waveguide for (a)  $w_d = 10$  nm, and (b)  $w_d = 50$  nm. Interference between waveguides for the metal barrier (c)  $w_m = 10$  nm and (d)  $w_m = 50$  nm. FDTD grid size was set to 1 nm.

On the other hand, too large value of  $w_d$  and  $w_m$  (composing large-width MIM waveguides) would result in fewer waveguide elements able to fit in the Fresnel lens; this could cause incomplete phase summation at the focal point as well as spatial quantization error. Coupling efficiency of the lens was thus calculated using FDTD for various values of  $w_d$  and  $w_m$ , above the minimum values obtained from the preceding analysis as shown in Fig. 4, with corresponding values of  $\beta_3$ ,  $l_0$ ,  $l_s$  and  $l_p$  obtained according to the dispersion relations (2) and formula (1).

Figure 5 shows coupling efficiencies of the metallic Fresnel lenses plotted as a function of  $w_d$  (25 ~200 nm) and  $w_m$  (30 ~70 nm), at the operating wavelength of 1550nm. Two sets of focal lengths,  $l_f = 1.5 \mu\text{m}$  (Fig. 5(a)) and  $l_f = 4 \mu\text{m}$  (Fig. 5 (a)), were tested to also investigate the performance and design parameters of the metallic Fresnel lens at different focal lengths. For the case of  $l_f = 1.5 \mu\text{m}$ , approximately 45% coupling efficiency (far better than that of the silicon Fresnel lens, 23%), and shorter working distance of  $2 \mu\text{m}$  was obtained with  $w_d = 50 \sim 100 \text{ nm}$ . For  $l_f = 4 \mu\text{m}$ , as much as 59% coupling efficiency (significantly improved compared to that of the silicon Fresnel lens, 27%) was achieved with  $w_d = 100 \sim 150 \text{ nm}$ . Worth to note, as observed in the figures, there existed relatively weaker dependencies on the thickness of the metal barrier  $w_m$ ; meanwhile, the optimum range of  $w_d$  was shifted for different focal lengths  $l_f$  of the lens. The relatively flat coupling efficiency around the optimum metal slit parameters will be beneficial in accommodating tolerances during hardware fabrication - such as employing metal stamping approach [24].

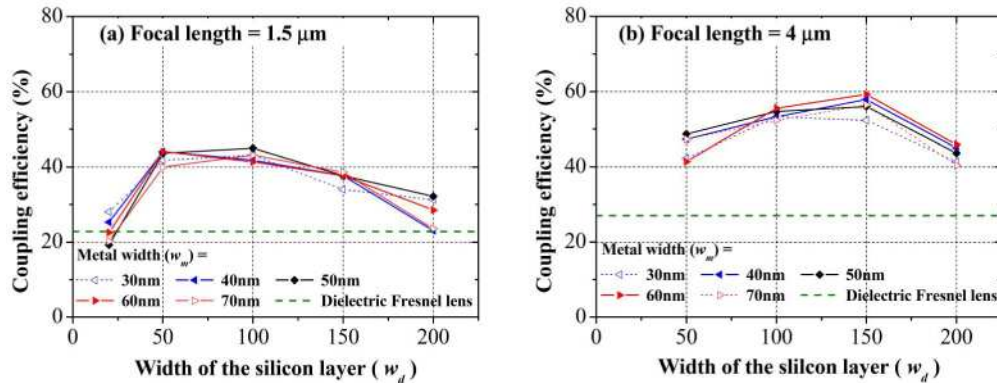


Fig. 5. Plot of coupling efficiencies for Fresnel lenses for focal lengths of (a)  $1.5 \mu\text{m}$  and (b)  $4 \mu\text{m}$  as a function of silicon dielectric width  $w_d$  and metallic barrier width  $w_m$ . Operation wavelength =  $1.55 \mu\text{m}$ .

#### 4. Conclusion

We investigated the feasibility of using Fresnel lens structures for nanophotonic coupling. Identifying the reflection problem associated with dielectric Fresnel lenses in wavelength scale coupler structures, we proposed a Fresnel lens with metal slit array to use plasmon propagation in the lens, to achieve significant enhancement in coupling efficiency as well a shorter, wavelength scale coupling length. Calculating phase evolution of plasmon in a MIM waveguide and then utilizing a phase array antenna formulation, we also derived the design principles for such a metallic Fresnel lens, and verified its operation with FDTD numerical analysis. Two sets of metallic Fresnel lens having different focal lengths were investigated in order to gain insight into their behavior, and to find the optimum design parameters for each lens. A direct coupling with excellent efficiency and order of wavelength coupling length, between beam sizes of vastly different dimensions ( $10 \mu\text{m}$  and  $0.36 \mu\text{m}$ ) was achieved. We expect our results to be useful in future integrated nanophotonic circuit applications.

#### Acknowledgements

This work was supported by the Korea Foundation for International Cooperation of Science & Technology (Global Research Laboratory project K2081500003), and in part by a Korea Science and Engineering Foundation (KOSEF) grant funded by the Korean government (MEST, R11-2008-095-01000-0).